J. Geogr. Sci. 2019, 29(11): 1876-1894
DOI: https://doi.org/10.1007/s11442-019-1994-y

Hydrochemical characteristics and controlling factors of natural water in the border areas of the Qinghai-Tibet Plateau

TIAN Yuan[1,2], *YU Chengqun[1], ZHA Xinjie[2,3], GAO Xing[3], DAI Erfu[1]

1. Lhasa National Ecological Research Station, Key Laboratory of Ecosystem Network Observation and Modelling, Institute of Geographic Sciences and Natural Resources Research, CAS, Beijing 100101, China;
2. University of Chinese Academy of Sciences, Beijing 100049, China;
3. State Key Laboratory of Resources and Environmental Information System, Institute of Geographic Sciences and Natural Resources Research, CAS, Beijing 100101, China

Abstract: The special geography and human environment of the Qinghai-Tibet Plateau has created the unique hydrochemical characteristics of the region's natural water, which has been preserved in a largely natural state. However, as the intensity of anthropogenic activities in the region has continued to increase, the water environment and hydrochemical characteristics of the Qinghai-Tibet Plateau have altered. In this study, water samples from the western, southern, and northeastern border areas of the Qinghai-Tibet Plateau, where human activities are ongoing, were collected, analyzed, and measured. The regional differences and factors controlling them were also investigated. The key results were obtained as follows. (1) Differences in the physical properties and hydrochemical characteristics, and their controlling factors, occurred in the different boundary areas of the Qinghai-Tibet Plateau. These differences were mainly the consequence of the geographical environment and geological conditions. (2) The water quality was good and suitable for drinking, with most samples meeting GB (Chinese national) and WHO (World Health Organization) drinking water standards. (3) The chemical properties of water were mainly controlled by the weathering of carbonates and the dissolution of evaporative rocks, with the former the most influential. (4) The biological quality indicators of natural water in the border areas were far superior to GB and WHO drinking water standards.

Keywords: border area of the Qinghai-Tibet Plateau; natural water; hydrochemical characteristics; controlling factors

Received: 2019-01-30 **Accepted:** 2019-03-20

Foundation: Key R&D and Transformation Program of Tibet, No.XZ201901NB08; Major Science and Technology Project of Tibet, No.XZ201901NA03, No.XZ201801NA02

Author: Tian Yuan (1991−), PhD, specialized in Tibet water environment and health. E-mail: tiany.13s@igsnrr.ac.cn

***Corresponding author:** Yu Chengqun (1965−), Professor and Ph.D. supervisor, specialized in Tibet agriculture and regional development. E-mail: yucq@igsnrr.ac.cn

1 Introduction

Water is the most active factor in the geographical environment. It interconnects and interacts with the atmosphere, biosphere, pedosphere, and lithosphere in a dynamic process of water circulation. Water quantity and quality constantly changes during this process. Moreover, the water environment surrounding habituated areas can directly or indirectly influence human life and development (Zheng *et al*., 2007). The Qinghai-Tibet Plateau (QT) is termed the "Headwater of Asia," as many rivers in China and Southeast Asia begin at the plateau. The area plays an important role in the protection and construction of national ecological security barriers, as freshwater has also become the most important strategic resource following energy resources (Sun *et al*., 2012). Because of environmental, transportation, and social historical development constraints, among others, the development level of water resources on the QT is lower than the average level in China. The QT is currently among the regions that are less affected by human activities and less polluted on earth. Its water environment still maintains a relatively complete native state (Tian *et al*., 2016). However, the special alpine environment makes the plateau ecological environment sensitive and extremely fragile. With the progress of society and the development of the economy, the instability of the ecological environmental system on the QT has increased along with the pressure on resources and the environment (Zhang *et al*., 2015).

At present, except for the uninhabited areas of the Qiangtang Plateau in the northern part of the QT, the degree of anthropogenic activities is increasing. Particularly, with the construction of the Xinjiang-Tibet Highway (on the western QT) and the Qinghai-Tibet Highway (on the northeastern QT), as well as the opening of the Zhangmu Port and the Jilong Port (on the southern QT), the QT is more frequently connected with the regions of southern Xinjiang in China, northwestern and southern China, and Nepal. Moreover, the boundary areas will gradually become an important channel for China to open to South Asia, an important pillar of the "the Belt and Road" strategy. This will further affect the environment of the plateau and its surrounding areas, changing the environment and hydrochemistry of the local natural water, which in turn will affect the production and life of local farmers and herdsmen. In recent years, research regarding the water chemistry on the QT has focused on the major rivers and lakes and their catchments, including Yarlung Zangbo (Sarin and Krishnaswami, 1984; Wang, 2016), Senge Zangbo (Li *et al*., 2012; Wang *et al*., 2012), Three River Resource areas (Deng, 1988; Wu *et al*., 2008; Cao, 2013; Tan *et al*., 2016), Qinghai Lake (Hou *et al*., 2009; Jin *et al*., 2009; Xiao *et al*., 2012), Yamzhog Yumco (Sun *et al*., 2012; Zhang *et al*., 2012; Sun *et al*., 2013; Zhe *et al*., 2017), Pumayum Co (Ju *et al*., 2010; Zhu *et al*., 2010), Nam Co (Gao *et al*., 2008; Guo *et al*., 2012; Wang *et al*., 2013), Mapam Yumco (Yao *et al*., 2015). Some scholars have also studied water chemistry in some areas of the QT (Zhang and Gustafsson, 1995; Guo and Wang, 2012; Tian *et al*., 2015), including microorganisms (Nie, 2011; Zhang *et al*., 2013; Zhao *et al*., 2017), heavy metals and trace elements (Cao *et al*., 2000; Grange *et al*., 2001; Li *et al*., 2006; Sheng *et al*., 2012; Tian *et al*., 2016).

However, the existing research lacks a systematic study of the hydrochemistry and the genesis of natural water in various boundary areas where human activities occur on the QT. The author collected water samples in the western, southern and northeastern boundary areas of the QT (Figure 1 and Table 1) and measured the physical properties on site during August,

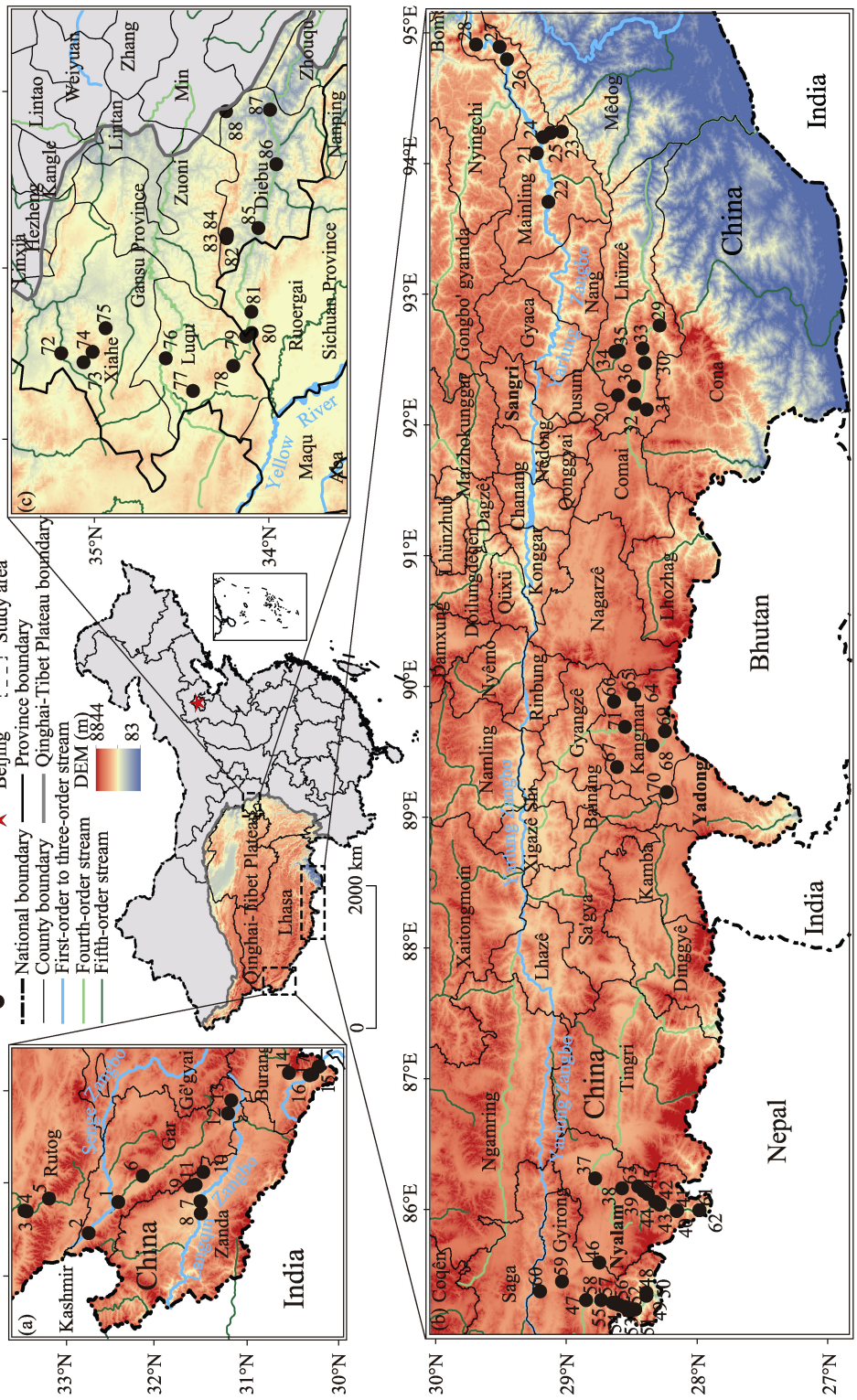

Figure 1 Geographical location of water sampling points in Qinghai-Tibet Plateau (QT): (a) water sampling points at western border area of QT; (b) water sampling points at southern border area of QT; (c) water sampling points at northeastern border area of QT

Table 1 Sampling points of water samples in the border areas of the Qinghai-Tibet Plateau

No.	Type	Town, County	Latitude (°)	Longitude (°)	Elevation (m)	No.	Type	Town, County	Latitude (°)	Longitude (°)	Elevation (m)
1	Well (14 m)	Zhaxigang, Gaer	32.3722	79.7976	4262	45	Stream	Yalai, Nyalam	28.4159	86.1307	4426
2	Stream	Zhaxigang, Gaer	32.6942	79.4597	4271	46	Stream	Borong, Nyalam	28.7547	85.5842	4643
3	Well (14 m)	Rituzong, Ritu	33.3922	79.7046	4264	47	Stream	Gyirong, Gyirong	28.3950	85.3294	2815
4	Well (15 m)	Risong, Ritu	33.3682	79.6971	4281	48	Stream	Gyirong, Gyirong	28.3952	85.3525	2731
5	Stream	Risong, Ritu	33.1262	79.8355	4359	49	Stream	Gyirong, Gyirong	28.4812	85.2251	3171
6	Stream	Kunsha, Gaer	32.1069	80.0823	4293	50	Stream	Gyirong, Gyirong	28.5006	85.2215	3261
7	Well (10 m)	Tuolin, Zhada	31.4778	79.8051	3712	51	Stream	Gyirong, Gyirong	28.5346	85.2195	3409
8	Well (8 m)	Tuolin, Zhada	31.4757	79.6732	3621	52	Stream	Gyirong, Gyirong	28.5418	85.2285	3510
9	Stream	Daba, Zhada	31.5879	79.9703	4582	53	Stream	Zongga, Gyirong	28.5635	85.2462	3632
10	Stream	Daba, Zhada	31.5314	79.9843	4493	54	Stream	Zongga, Gyirong	28.6056	85.2599	3760
11	Stream	Daba, Zhada	31.4484	80.1229	4693	55	Stream	Zongga, Gyirong	28.6301	85.2691	3736
12	Stream	Menshi, Gaer	31.1789	80.7601	4450	56	Stream	Zongga, Gyirong	28.6533	85.2781	3785
13	Stream	Menshi, Gaer	31.1426	80.9014	4636	57	Stream	Zongga, Gyirong	28.7397	85.2965	3955
14	Well (10 m)	Pulan, Pulan	30.2945	81.1759	3905	58	Stream	Zongga, Gyirong	28.8557	85.2968	4145
15	Well (5 m)	Kejia, Pulan	30.1927	81.2707	3734	59	Stream	Zheba, Gyirong	29.0409	85.4394	4733
16	Stream	Kejia, Pulan	30.2633	81.1870	3891	60	Stream	Zheba, Gyirong	29.2074	85.3636	4527
17	Stream	Namumani, Pulan	30.5157	81.2018	4521	61	Stream	Zhangmu, Nyalam	27.9887	85.9828	2277
18	Stream	Huoer, Pulan	30.6872	81.8323	4752	62	Stream	Zhangmu, Nyalam	27.9903	85.9829	2263
19	Stream	Longzi, Longzi	28.4081	92.4628	3881	63	Stream	Yalai, Nyalam	28.3828	86.1070	4373
20	Stream	Ridang, Longzi	28.6125	92.2153	4998	64	Stream	Nierudui, Kangma	28.4865	89.9269	4569
21	Stream	Zhaxiraodeng, Milin	29.2319	94.0680	2993	65	Stream	Nierudui, Kangma	28.4894	89.9265	4584
22	Stream	Wolong, Milin	29.1447	93.6939	3032	66	Stream	Nierumai, Kangma	28.6419	89.8728	4389
23	Stream	Nanyi, Milin	29.1849	94.1883	2938	67	Stream	Zhangxiong, Kangma	28.6183	89.3708	4489
24	Stream	Nanyi, Milin	29.1279	94.2226	3009	68	Stream	Samada, Kangma	28.3495	89.5377	4447
25	Stream	Nanyi, Milin	29.0417	94.2321	3147	69	Stream	Samada, Kangma	28.2517	89.6455	4573

(*To be continued on the next page*)

(*Continued*)

No.	Type	Town, County	Latitude (°)	Longitude (°)	Elevation (m)	No.	Type	Town, County	Latitude (°)	Longitude (°)	Elevation (m)
26	Stream	Danniang, Milin	29.4613	94.7849	2945	70	Stream	Gala, Kangma	28.2388	89.1817	4474
27	Stream	Pai, Milin	29.5174	94.8811	2931	71	Stream	Kangma, Kangma	28.5587	89.6807	4298
28	Stream	Pai, Milin	29.6977	94.8978	2821	72	Stream	Labuleng, Xiahe	35.1936	102.5151	2942
29	Stream	Jiayu, Longzi	28.2941	92.7492	3380	73	Stream	Sangke, Xiahe	35.0651	102.4624	3207
30	Stream	Liemai, Longzi	28.4247	92.5742	3851	74	Stream	Sangke, Xiahe	35.0126	102.5232	3399
31	Stream	Ridang, Longzi	28.3930	92.1056	4253	75	Stream	Sangke, Xiahe	34.9377	102.6594	3249
32	Stream	Ridang, Longzi	28.4883	92.2845	4119	76	Stream	Maai, Luqu	34.5901	102.4854	3112
33	Stream	Xuesha, Longzi	28.6346	92.5459	4245	77	Stream	Gahai, Luqu	34.4331	102.2976	3432
34	Stream	Xuesha, Longzi	28.6337	92.5489	4175	78	Stream	Gahai, Luqu	34.2006	102.4419	3491
35	Stream	Xuesha, Longzi	28.6038	92.5566	3905	79	Stream	Benzilan, Luqu	34.1269	102.6116	3358
36	Stream	Rerong, Longzi	28.4856	92.1489	4064	80	Stream	Langmu, Luqu	34.0949	102.6318	3393
37	Well (8 m)	Menbu, Nyalam	28.7857	86.2255	4452	81	Stream	Hongxing, Nuoergai	34.0959	102.7545	3161
38	Stream	Menbu, Nyalam	28.5812	86.1501	4857	82	Stream	Zhagana, Diebu	34.2394	103.1792	2974
39	Stream	Yalai, Nyalam	28.4565	86.1650	4560	83	Stream	Zhagana, Diebu	34.2374	103.2025	2978
40	Stream	Nyalam, Nyalam	28.1598	85.9805	3771	84	Stream	Zhagana, Diebu	34.2370	103.1979	2939
41	Stream	Nyalam, Nyalam	28.1634	85.9768	3788	85	Stream	Dianga, Diebu	34.0558	103.2373	2355
42	Stream	Yalai, Nyalam	28.2928	86.0248	4104	86	Stream	Wangzang, Diebu	33.9520	103.6059	2007
43	Stream	Yalai, Nyalam	28.3273	86.0474	4259	87	Stream	Huayuan, Diebu	33.9885	103.9207	1733
44	Stream	Yalai, Nyalam	28.3828	86.1070	4373	88	Stream	Sigou, Minxian	34.2426	103.9113	2948

October and November 2017. During September and December of 2017, the author analyzed and tested the elemental contents of the water at the Physical and Chemical Analysis Center of the Institute of Geographic Sciences and Natural Resources Research, Chinese Academy of Sciences (IGSNRR, CAS). Based on the collection and analysis of water samples from the three boundary areas of the QT, the hydrochemistry and causes of natural waters in different boundary areas of the QT were studied, and a comparison of regional differences between different boundary areas was completed.

2 Materials and methods

2.1 Study area

The QT has a land area of 2.57×10^6 km^2 (26.0033°–39.7806°N, 73.3144°–104.7831°E) along the southwestern border of China, with an average elevation higher than 4000 m above sea level (Zhang *et al*., 2002). The northeastern border areas of the QT are in the transitional zone between the QT and the Loess Plateau. The terrain is higher in elevation to the northwest (meadow steppe) and lower to the southeast (the Min-Die mountain area). The southern border areas are in the Himalayas and the geomorphological type is mainly deep-cutting alpine gorge and plateau strath lake basin. The western border areas are on the western Qiangtang Plateau, where the Kunlun Mountains, Gangdese Mountains, and Himalayas are distributed to the north, central, and south, respectively. Here, the geomorphological type is mainly plateau lake basin, river valley, terrestrial forest, and alpine gully. Since the Proterozoic, the strata of the system have been well developed, and the sedimentary rock types are diverse atop the QT, particularly the well-exposed Mesozoic–Cenozoic marine strata. Igneous rocks and metamorphic rocks are widely distributed, various rock types are exposed, and the rock types are complex (Lu *et al*., 2016). Rainfall and runoff are abundant to the east and south, and the supply of surface water and groundwater is sufficient; however, the climate to the west and north is arid, comprising a global cold and arid core. The average annual precipitation of each boundary sampling county is approximately 620 mm (northeastern boundary), 570 mm (southern boundary), and 130 mm (western boundary), respectively (NBS, 2017). In 2016, the county gross domestic product (GDP) of prefecture-level cities in the border areas of the QT was 1.707 billion yuan (along the northeastern border; Gannan Tibetan Autonomous Prefecture), 1.12 billion yuan (along the southern border; Shigatse City, Shannan City, and Nyingchi City), and 604 million yuan (along the eastern border, Ali (Ngari) Prefecture), respectively (NBS, 2017).

2.2 Field measurement

The location at each collection sample recorded the coordinate by using a handheld GPS (Global Position System) device (equipment model: 530HCx, produced by GARMIN). The pH, Ec (electrical conductivity) and T (temperature) were in-situ tested by using a pH tester (Limit of detection (LOD): 0.01, equipment model: SX-620, produced by Sanxing, Shanghai) and Ec tester (LOD: 0.1 μS/cm, equipment model: SX-650, produced by Sanxing, Shanghai) respectively. The TDS (total dissolved solids) were automatically converted by the instrument through Ec. Collection and preservation of all water samples are followed the Standard Examination Methods for Drinking Water (GB/T 5750-2006) (MH, 2007).

2.3 Laboratory analysis method

The bicarbonate (CO_3^{2-}) and carbonate (HCO_3^-) were analyzed using an acid-base titration according to the method of Ministry of Health (MH) of the P.R.C. (MEP, 2002; MH, 2007). Anions of chlorine (Cl^-), sulfate (SO_4^{2-}), nitrate (NO_3^-), fluorine (F^-), phosphate (PO_4^{3-}) and nitrite (NO_2^-) were analyzed using IC (Ion Chromatography, LOD: 0.001 mg/L, equipment model: ICS-900, produced by Thermo Fisher Scientific) at the IGSNRR, following the U.S. Environmental Protection Agency (EPA) method 300.0 (EPA, 1993). Major cations of calcium (Ca^{2+}), potassium (K^+), magnesium (Mg^{2+}), sodium (Na^+) and silicon (Si) were deter-

mined using ICP-OES (Inductively Coupled Plasma Optical Emission Spectrometry, LOD: 0.001 mg/L, equipment model: Optima 5300 DV, produced by PerkinElmer). Quality assurance were controlled by using certified external standard solutions and retested sample measurements (retest 1 sample after run every 10 samples) during the analysis to ensure and verify the stability of the results. Certified external standard of cations solutions for Ca^{2+}, K^{+}, Mg^{2+}, Na^{+}, and Si were prepared from Multi-element ICP-MS calibration standards (No.Lot# 15-76JB and Cat# N9300233). Certified external standard of anions solutions were prepared from GB of F^{-} (GBW080549), Cl^{-} (GBW080268), SO_4^{2-} (GBW080266), PO_4^{3-} (GBW080435), NO_3^{-} (GBW080264) and NO_2^{-} (GBW080223), respectively.

The relative error of total anion and cation (equivalent ratio) in 88 samples ranged from 0.01% to 4.67%, less than 5.00% (Figure 2). Therefore, it can be said that the total anion and cation in the measured water are basically balanced (Shen *et al*., 1993), i.e., our data are accurate and reliable.

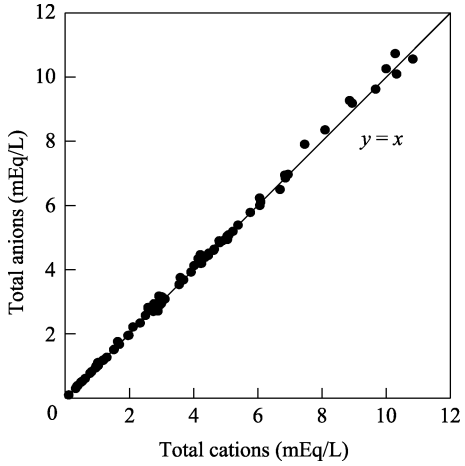

Figure 2 Total cation (mEq/L) and total anion (mEq/L) relative error of water samples on the Qinghai-Tibet Plateau

3 Results and discussion

3.1 Elements concentrations

The water samples of QT border areas have suitable hydrochemical characteristics (Table 2). The pH value ranged from 6.52 to 8.88 (mean value: 7.75), and the TDS ranged from 6.11 mg/L to 583 mg/L (mean value: 180 mg/L). The TH (hardness) of the QT border area water samples was calculated, ranging between 3.69 mmol/L and 512 mmol/L (mean value: 168 mmol/L).

Significant spatial variations in the major cations and anions indicate the impact of different lithologies and anthropogenic activities at a watershed scale (Li and Zhang, 2008). The statistical data (min, max, mean, median, SD, skewness) for the major elemental composition of the water samples in different QT border areas are listed in Table 2. The water samples major cations relative concentration order is $K^{+} < Mg^{2+} < Na^{+} < Ca^{2+}$ (in the western QT border area) and $K^{+} < Na^{+} < Mg^{2+} < Ca^{2+}$ (in the southern and northeastern QT border areas), while order of the anions in water samples is $NO_3^{-} < Cl^{-} < SO_4^{2-} < HCO_3^{-}$ (in the western QT border area) and $NO_3^{-} < Cl^{-} < SO_4^{2-} < HCO_3^{-}$ (in the southern and northeastern QT border areas) (Table 2). The lowest TDS and TH of the water samples on the QT was found in the western border area, with a mean value of 142.01 mg/L and 122.55 mg/L respectively.

Natural water in different QT border areas is mainly fresh-soft water and fresh-hard water. No water samples in the QT border areas with high TDS (> 1000 mg/L) and TH (> 1000 mg/L) were classified as brackish-hard water (Figure 3). Most water samples from western border of the QT were fresh-soft water, but water samples from the northeastern border of the QT were fresh-hard water (Figure 3).

Table 2 Parameters and elements concentration statistical summary of the water samples of the Qinghai-Tibet Plateau border areas

Parameters		pH	TDS	TH	Ca^{2+}	K^{+}	Mg^{2+}	Na^{+}	HCO_3^{-}	Cl^{-}	SO_4^{2-}	NO_3^{-}	Si
Unit			mg/L	mmol/L	mg/L	mg/L	mg/L	mg/L	mg/L	mg/L	mg/L	mg/L	mg/L
All	Min	6.52	6.11	3.69	1.10	0.00	0.19	0.19	2.95	0.00	1.29	0.00	2.08
	Max	8.88	583	512	149	8.43	71.0	32.8	305	21.7	356	32.2	20.7
	Mean	7.75	180	168	44.7	1.03	13.5	6.06	127	2.33	59.2	2.60	8.77
	Median	7.75	171	143	42.3	0.87	9.02	3.75	109	0.68	28.7	1.15	7.64
	SD	0.50	130	127	30.9	1.06	14.6	6.30	95.8	3.98	80.8	4.48	4.10
	Skewness	–0.04	1.13	0.88	0.77	3.89	1.75	1.66	0.37	2.94	2.03	4.33	0.85
West	Min	6.99	32.9	27.6	9.38	0.00	0.99	0.19	16.4	0.00	3.48	0.00	4.85
	Max	8.88	391	394	69.3	8.43	52.9	32.8	302	21.7	199	32.2	20.7
	Mean	8.38	142	122	31.0	1.44	10.6	10.8	106	5.62	46.9	3.41	10.2
	Median	7.74	171	146	42.4	0.86	9.09	3.54	108	0.67	29.6	1.17	7.50
	SD	0.44	79.1	82.8	17.4	1.77	11.1	8.37	70.1	6.79	45.0	7.42	4.96
	Skewness	–1.97	1.45	1.76	0.54	3.37	2.95	0.74	0.92	1.08	2.13	3.23	0.75
South	Min	6.52	6.11	3.69	1.10	0.00	0.19	0.38	2.95	0.31	1.29	0.40	2.08
	Max	8.07	583	512	149	2.72	58.7	23.7	305	9.84	356	19.2	18.3
	Mean	7.57	187	163	44.5	0.77	12.5	4.32	98.6	0.96	74.4	1.74	8.46
	Median	7.66	131	128	38.4	0.64	5.30	3.02	74.3	0.57	38.3	1.04	6.95
	SD	0.36	156	146	36.0	0.68	15.2	4.68	90.6	1.68	95.7	2.71	4.04
	Skewness	–1.11	0.92	0.90	0.85	0.76	1.44	1.92	0.93	4.47	1.51	5.30	0.68
Northeast	Min	6.87	119	148	40.6	0.34	4.44	0.99	162	0.97	3.35	0.92	3.51
	Max	8.14	330	462	81.9	2.87	71.0	20.6	298	12.4	139	16.3	14.0
	Mean	7.66	198	231	59.9	1.40	19.5	6.50	238	3.11	24.5	4.38	8.22
	Median	7.77	198	224	58.1	1.00	17.1	4.34	250	2.54	15.7	2.09	8.04
	SD	0.40	47.7	66.8	12.0	0.76	14.4	5.48	37.2	2.58	31.2	3.96	2.64
	Skewness	–0.68	0.91	2.27	0.14	0.47	2.54	1.55	-0.28	2.70	2.90	1.59	0.34

Note: SD means standard deviation

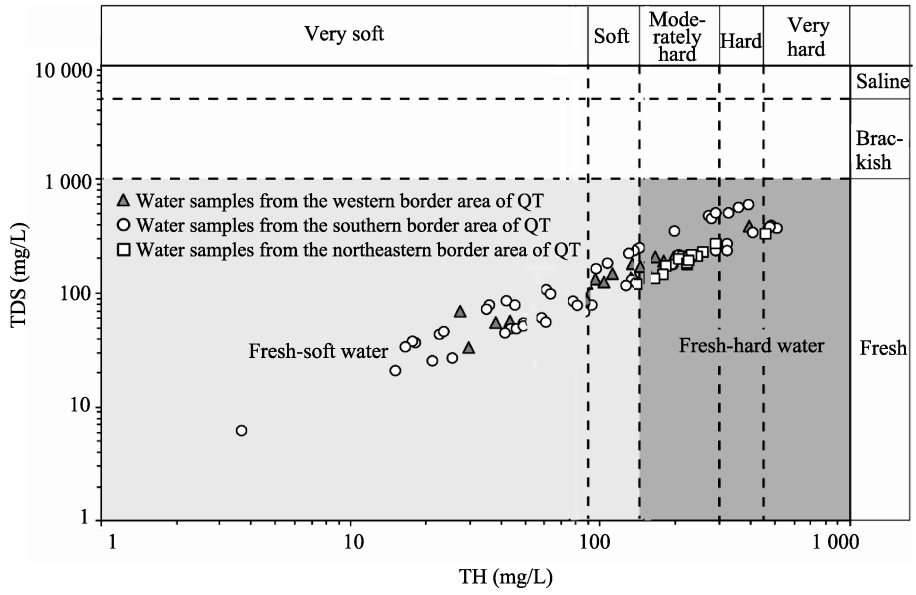

Figure 3 Water quality of water samples in different border areas of the Qinghai-Tibet Plateau

In Table 3, TDS, Ca^{2+}, Mg^{2+}, Na^{+}, and Cl^{-} in all of the water samples of QT border areas were less than the drinking water standards of both GB and WHO. The pH value of all the water samples meets the WHO drink water standard and all the water samples of southern and northeastern QT border areas meet both standards. However, only 50% of the water samples from the western border of the QT meet the GB standard (Table 3), while 7.5% and 5.9% of the water samples in the southern and northeastern QT border areas exceed the GB TH standard, respectively. Only one water sample in the QT southern border area exceeds the WHO drinking water standard (Table 3). Approximately 11% of the water samples in the southern QT border areas exceed the SO_4^{2-} value of the two drinking water standards. The NO_3^{-} value of all the water samples meets the GB and WHO drinking water standards. Therefore, the majority of the natural water in the border areas of the QT is suitable for drinking.

Table 3 Distribution of water samples exceeding the drinking water standards in border areas of the Qinghai-Tibet Plateau

Parameters	GB	WHO	Number of exceeding the drinking water standards		
	(MH 2007)	(WHO 2008)	West	South	Northeast
pH	6.5–8.5	6.5–9.5	9 (50%)	0	0
TDS	1000	1000	0	0	0
TH	450	500	0	4 (7.5%)	1 (5.9%)
Ca^{2+}	–	300	0	0	0
Mg^{2+}	–	300	0	0	0
Na^{+}	200	200	0	0	0
Cl^{-}	250	250	0	0	0
SO_4^{2-}	250	250	0	6 (11%)	0
NO_3^{-}	44	50	0	0	0

Note: GB means Chinese State Standard

3.2 Hydrochemical characteristics

The relative amounts of major anions and cations in water samples of the QT border area are shown by using a Piper diagram; the hydrochemical characteristics of water was determined by the percentage of major anions and cations (Piper, 1944).

The QT border water samples are dominated by Ca^{2+}–Mg^{2+}–HCO_3^{-} (n=19), Ca^{2+}–Mg^{2+}–HCO_3^{-}– SO_4^{2-} (n=13), Ca^{2+}–Mg^{2+}–SO_4^{2-}–HCO_3^{-} (n=13), Ca^{2+}–HCO_3^{-} (n=13) and Ca^{2+}–HCO_3^{-}– SO_4^{2-} (n=10), with an average pH of 7.75 (Table 2). In different water samples, some observations are as follows: (1) Most water samples of the western border are weakly alkaline (average pH is 8.38) (Table 2); Ca^{2+}–Mg^{2+}–HCO_3^{-}–SO_4^{2-} (n=4) and Ca^{2+}–Mg^{2+}– SO_4^{2-}–HCO_3^{-} (n=2) are the most common water types. (2) Most water samples of the southern border are slightly alkaline (average pH is 7.57) (Table 2); Ca^{2+}–Mg^{2+}–SO_4^{2-}– HCO_3^{-} (n=11), Ca^{2+}–Mg^{2+}–HCO_3^{-}– SO_4^{2-} (n=9), Ca^{2+}–HCO_3^{-}–SO_4^{2-} (n=9), Ca^{2+}–Mg^{2+}– HCO_3^{-} (n=7), and Ca^{2+}–HCO_3^{-} (n=7) are the most common water types of these water samples. (3) Most water samples of the northeastern border are slightly alkaline (average pH is 7.66) (Table 2); Ca^{2+}–Mg^{2+}–HCO_3^{-} (n=11) and Ca^{2+}–HCO_3^{-} (n=4) are the most common water types (Figure 4).

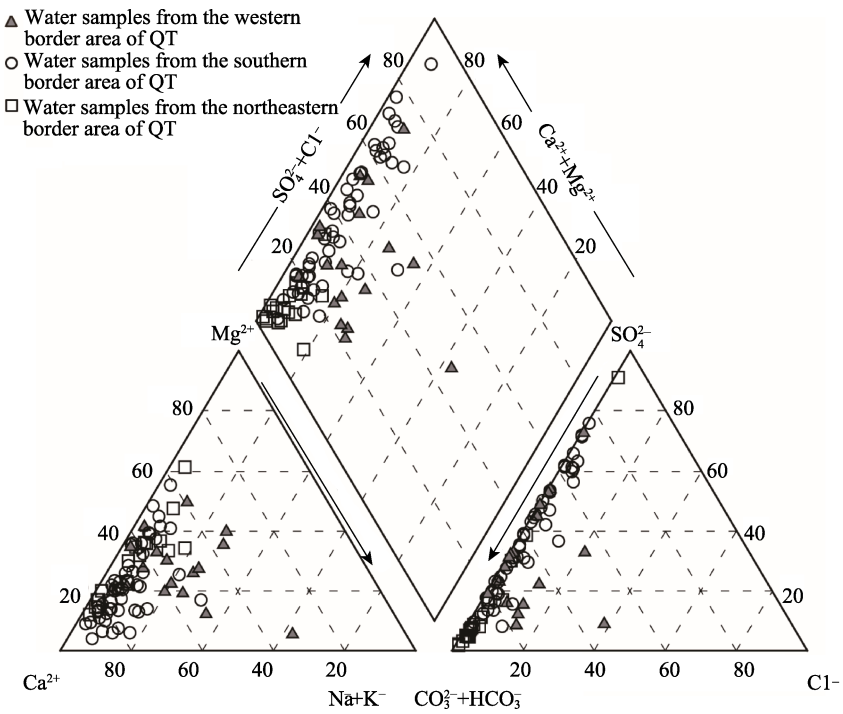

Figure 4 Piper diagrams for water samples from different border areas of the Qinghai-Tibet Plateau

3.3 Preliminary discussion of ion sources

Gibbs boomerang envelope (Gibbs, 1970) built a simple model by using the TDS values versus the $Na^+/(Na^+{+}Ca^{2+})$ (weight ratio) and the TDS values versus $Cl^-/(Cl^-{+}HCO_3^-)$ (weight ratio) measuring the relative significance of the three types of natural factors (evaporation, weathering, and precipitation) that control surface water chemistry.

The Gibbs model plot shows that the rock weathering controls the main hydrochemical composition in the QT border areas (Figure 5), basically consistent with the previous study of rivers on the QT (Zhu *et al*., 2010; Yao *et al.,* 2015; Zhe *et al*., 2017).

3.4 Mechanisms controlling hydrochemistry

A total of 11.6% of global river solutes originate from silicates, 17.2% from evaporites (although evaporites only account for approximately 1.25% of the surface rock distribution area), and approximately 50% from carbonates (Meybeck, 1987). The major anions and cations in water which have been weathered from stratum and dissolved in water can determine the rock type, e.g., Ca^{2+} and Mg^{2+} may originate from carbonates, evaporites, or silicates; Na^+ and K^+ from both evaporites and silicates; Cl^- and SO_4^{2-} mainly from the dissolution of evaporites; and HCO_3^- mostly from weathered carbonates (Li and Zhang, 2008).

The milliequivalent (mEq) ratio of $Cl^-{+}SO_4^{2-}$ to HCO_3^- in the QT water samples from the western and southern border areas is approximately equal to 1 (Figure 6a). The mEq ratios of $Ca^{2+}{+}Mg^{2+}$ to HCO_3^- (Figure 6b) and $Ca^{2+}{+}Mg^{2+}$ to SO_4^{2-} (Figure 6c) are greater than 1. The mEq ratio of $Ca^{2+}{+}Mg^{2+}$ to $HCO_3^-{+}SO_4^{2-}$ is approximately equal to 1 (Figure 6d). This indicates that the ions in these water samples are mainly controlled by the carbonate weathering

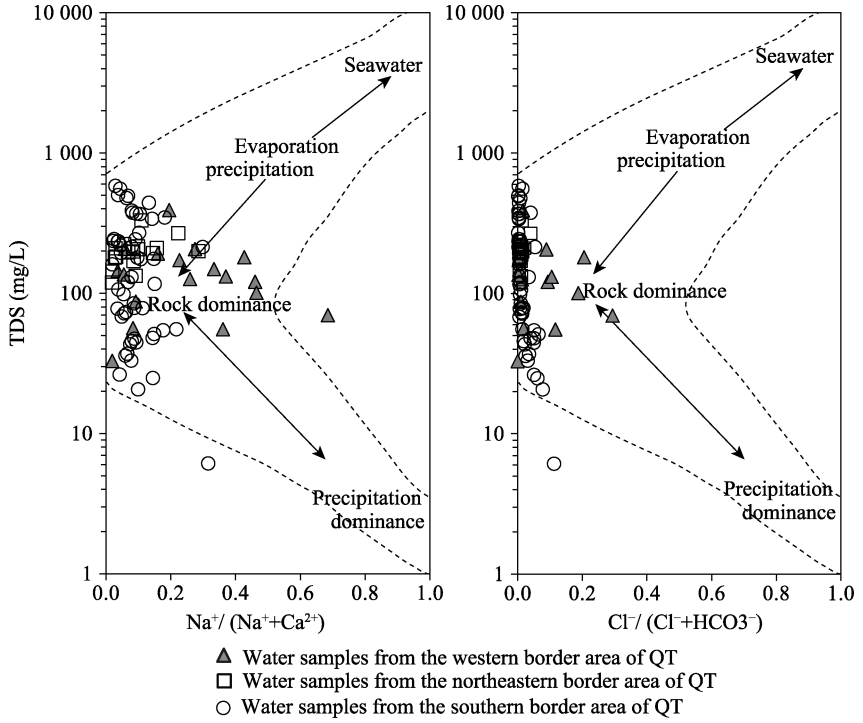

Figure 5 Gibbs boomerang envelope model plot

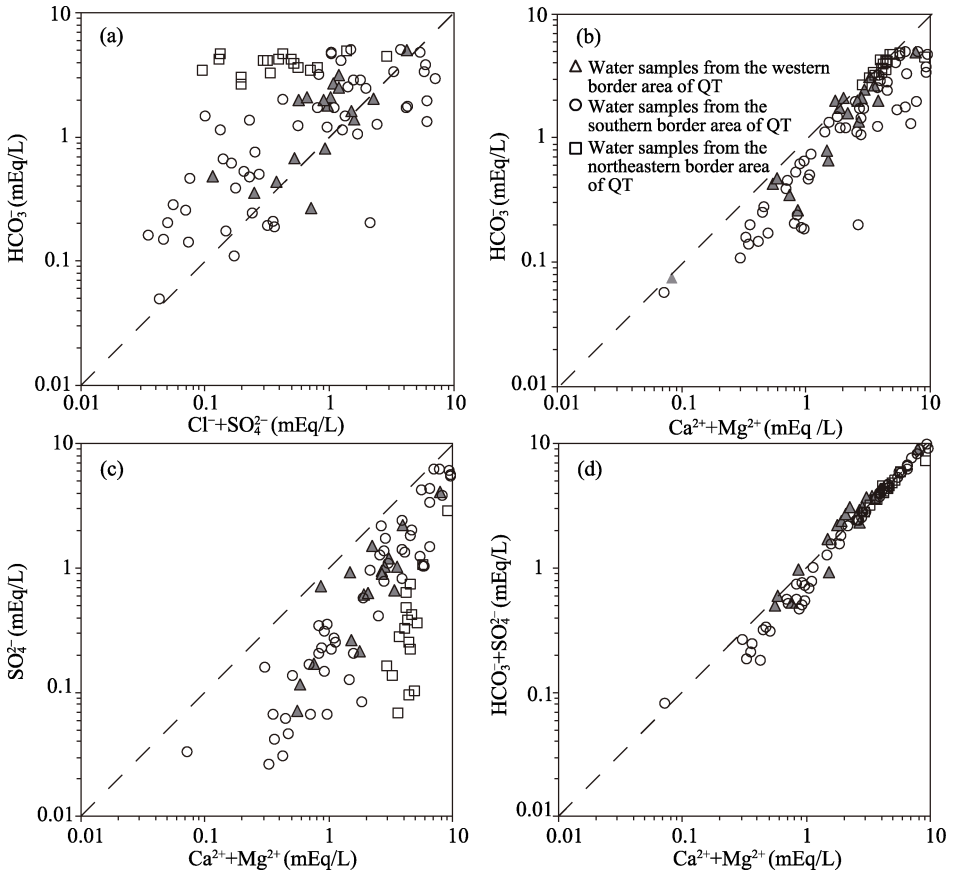

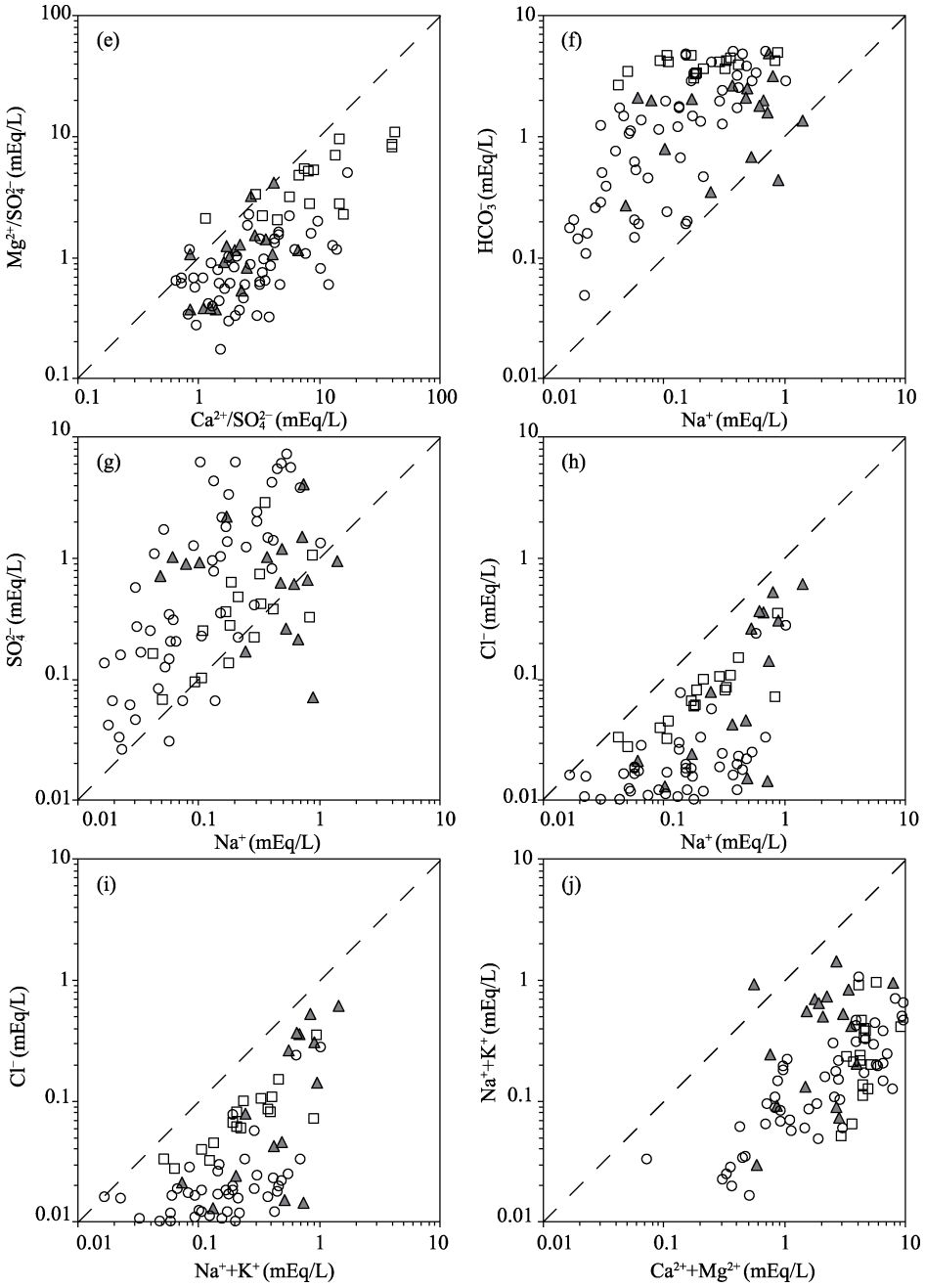

Figure 6 Scatter diagrams of (a) $Cl^- + SO_4^{2-}$ and HCO_3^-, (b) $Ca^{2+} + Mg^{2+}$ and HCO_3^-, (c) $Ca^{2+} + Mg^{2+}$ and SO_4^{2-}, (d) $Ca^{2+} + Mg^{2+}$ and $HCO_3^- + SO_4^{2-}$, (e) Ca^{2+}/SO_4^{2-} and Mg^{2+}/SO_4^{2-}, (f) Na^+ and HCO_3^-, (g) Na^+ and SO_4^{2-}, (h) Na^+ and Cl^-, (i) $Na^+ + K^+$ and Cl^-, (j) $Ca^{2+} + Mg^{2+}$ and $Na^+ + K^+$ for the water samples in different border area of the Qinghai-Tibet Plateau

and the dissolution of evaporites. This further suggests the weathering of carbonate mineral (e.g., calcite and dolomite) and dissolution of sulfate mineral (e.g., gypsum) could be crucial reactions resulting in the Ca^{2+} and Mg^{2+} in water (Dalai *et al*., 2002). Meanwhile, the mEq ratios of Ca^{2+}/SO_4^{2-} to Mg^{2+}/SO_4^{2-} (Figure 6e) in most of the water samples are slightly

greater than 1, meaning the content of Ca^{2+} is higher than that of Mg^{2+} and the sulfate dissolution contribution is less than that of carbonates weathering (Li and Zhang, 2008). In the water samples from the northeastern border area of the QT, the mEq ratio of $Cl^-+SO_4^{2-}$ to HCO_3^- (Figure 6a) is much less than 1, the mEq of $Ca^{2+}+Mg^{2+}$ is nearly equal in proportion to HCO_3^- (Figure 6b), and the mEq ratio of $Ca^{2+}+Mg^{2+}$ to SO_4^{2-} (Figure 6c) is much greater than 1, indicating that the Ca^{2+} and Mg^{2+} in the QT border areas water samples is closely related to HCO_3^-. The ions (their types and concentrations) are mainly controlled by carbonate weathering; and the Ca^{2+} and Mg^{2+} may originate from the weathering of carbonate minerals (e.g., calcite and dolomite).

The mEq ratio of Na^+ to HCO_3^- (Figure 6f) in most of the water samples is less than 1, while the mEq ratio of Na^+ to SO_4^{2-} (Figure 6g) in the western and northeastern border area water samples is approximately equal to 1, suggesting that the dissolution of sulfate minerals (e.g., mirabilite) may be among the sources of Na^+ in the water samples of western and northeastern areas (Zhe *et al*., 2017). Meanwhile, the mEq ratio of Na^+ to SO_4^{2-} (Figure 6g) in the southern area water samples is less than 1. Therefore, the Na^+ in the southern border area water samples may originate from silicates (Zhe *et al*., 2017). Generally, the ratio of Na^++K^+ to Cl^- is equal to 1 when the dissolution of evaporites plays a major role in hydrochemical compositions (Gibbs, 1970). Both the mEq ratios of Na^+/Cl^- (Figure 6h) and $(Na^++K^+)/Cl^-$ (Figure 6i) are greater than 1, indicating that halite in evaporites (e.g., NaCl and KCl) are the main source of Cl^- in the water samples.

The ratio of $(Ca^{2+}+Mg^{2+})/(Na^++K^+)$ in the water can be used as an indicator to distinguish the relative intensity of different rock weathering. Silicate weathering releases more Na^++K^+ than $Ca^{2+}+Mg^{2+}$ (Sarin *et al*., 1989). Relatively high $(Ca^{2+}+Mg^{2+})/(Na^++K^+)$ (Figure 6j) and SO_4^{2-}/Na^+ (Figure 6g) ratios indicate that the rocks are rich in Ca^{2+}, Mg^{2+} and SO_4^{2-} (e.g., gypsum and dolomite) on the water sample hydrochemistry. The world's rivers average ratio of $(Ca^{2+}+Mg^{2+})/(Na^++K^+)$ is 2.2 (Meybeck and Helmer 1989). Carbonate weathering may cause the high ratio of $(Ca^{2+}+Mg^{2+})/(Na^++K^+)$ in a river/stream, such as the Lake Qinghai catchment in China which ranges from 5.5–20.3 (Hou *et al*., 2009), the carbonate bedrock section of Ganges-Brahmaputra River in India which ranges from 5.2–11.5 (Sarin and Krishnaswami, 1984), the Yangtze River in China which is 5.1 (Chen *et al*., 2002), the Indus River in India which is 6 (Ahmad *et al*., 1998) and the Mackenzie River in Canada which is 6.9 (Reeder *et al*., 1972). Conversely, the low ratio of $(Ca^{2+}+Mg^{2+})/(Na^++K^+)$ in a river/stream means it is probably controlled by the dissolution of evaporites, such as rivers around the Taklimakan Desert which are approximately 0.9 (Zhu and Yang, 2007), the Orinoco River in South America which is 1.5 (Nemeth *et al*., 1982) and the Buha–Heima River of the Lake Qinghai catchment which ranges from 1.36–6.81 (Hou *et al*., 2009). The QT border area water samples average ratio of $(Ca^{2+}+Mg^{2+})/(Na^++K^+)$ decreases in the following order: northeastern (23.8) > southern (18.2) > western (9.8). This means that the process of carbonate weathering in the water has intensifies from the western to eastern QT.

3.5 Anthropogenic input

The hydrochemical characteristics of water can be affected by human activities (Meybeck and Helmer, 1989; Katz *et al*., 2001). Because of the rapid increase in industrial and agricultural activities, this impact has recently become significant in whole China (Chen *et al*.,

Table 4 Values of anthropogenic input geochemical variables in water compared with GB and WHO drinking water standards

Parameter	Border area of QT			GB	WHO
	Western	Southern	Northeastern	(MH 2007)	(WHO 2008)
NO_2^- (mg/L)	n.a.	0.02	0.08	–	3
NO_3^- (mg/L)	3.41	1.71	4.38	44	50
SO_4^{2-} (mg/L)	46.91	74.45	24.53	250	250
PO_4^{3-} (mg/L)	n.a.	n.a.	n.a.	–	–

n.a. (not applicable) means the concentration of parameter is lower than the LOD or is not detected.

2002). Generally, non-point source pollutants (i.e. fertilization) and surficial geological function (i.e. weathering) are the two important sources of NO_3^- (Holloway *et al*., 1998). The presence of biogenic substances such as nitrogen, sulfur, and phosphorus compounds (e.g., NO_2^-, NO_3^-, SO_4^{2-}, and PO_4^{3-}) in natural water can reflect the impact of human activities on the chemical composition of water, to some extent (Roy *et al*., 1999).

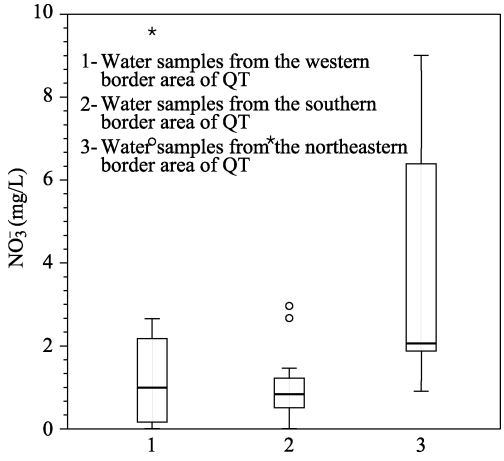

Figure 7 Box and whisker plot of water nitrate concentrations in different border areas of the Qinghai-Tibet Plateau

The average nitrogen compounds in the order from the lowest to the highest are as follows (Table 4 and Figure 7): northeast > west > south. This order basically coincides with the socio-economic development in these areas. The average sulfur compounds have a general trend of south > east > west (Table 4). Phosphorus compounds in all the QT water samples were less than the limit of detection or were not detected (Table 4). One can see from Table 4 that all the biogenic substances in the water samples are very low and far lower than GB and WHO drinking water standards, indicating the QT is less affected by human activities.

3.6 Spatial pattern of major ions

Principal component analysis (PCA) of hydrochemical characteristics parameters derived three significant factors (Table 5). The percentages of variance indicate three components accounting for approximately 85.34%, 75.40%, and 80.61% of the total variability water samples in the western, southern, and northeastern QT border areas, respectively. The scores of variables on the principal component vector are plotted in Figure 8.

PCA (Table 5, Figures 8a and 8b) of the western QT border area water samples shows strong relationships in the first component between Ec, TDS, TH, Ca^{2+}, Mg^{2+}, K^+, SO_4^{2-}, and HCO_3^-, which indicate the carbonate weathering and evaporite dissolution (Gibbs, 1970; Chen *et al*., 2002). The relationships between Na^+, Cl^-, NO_3^-, and SiO_2 in the second component reflect the silicate weathering, evaporite dissolution, and some anthropogenic input (Gibbs, 1970; Cruz and Amaral, 2004). Because of the minimal amount of precipitation and human activities, silicate contributes more to the western QT (Yao *et al*., 1996; Chang *et al*., 2012). The F^- shows the dominant nature in the third component (Figure 8b), which

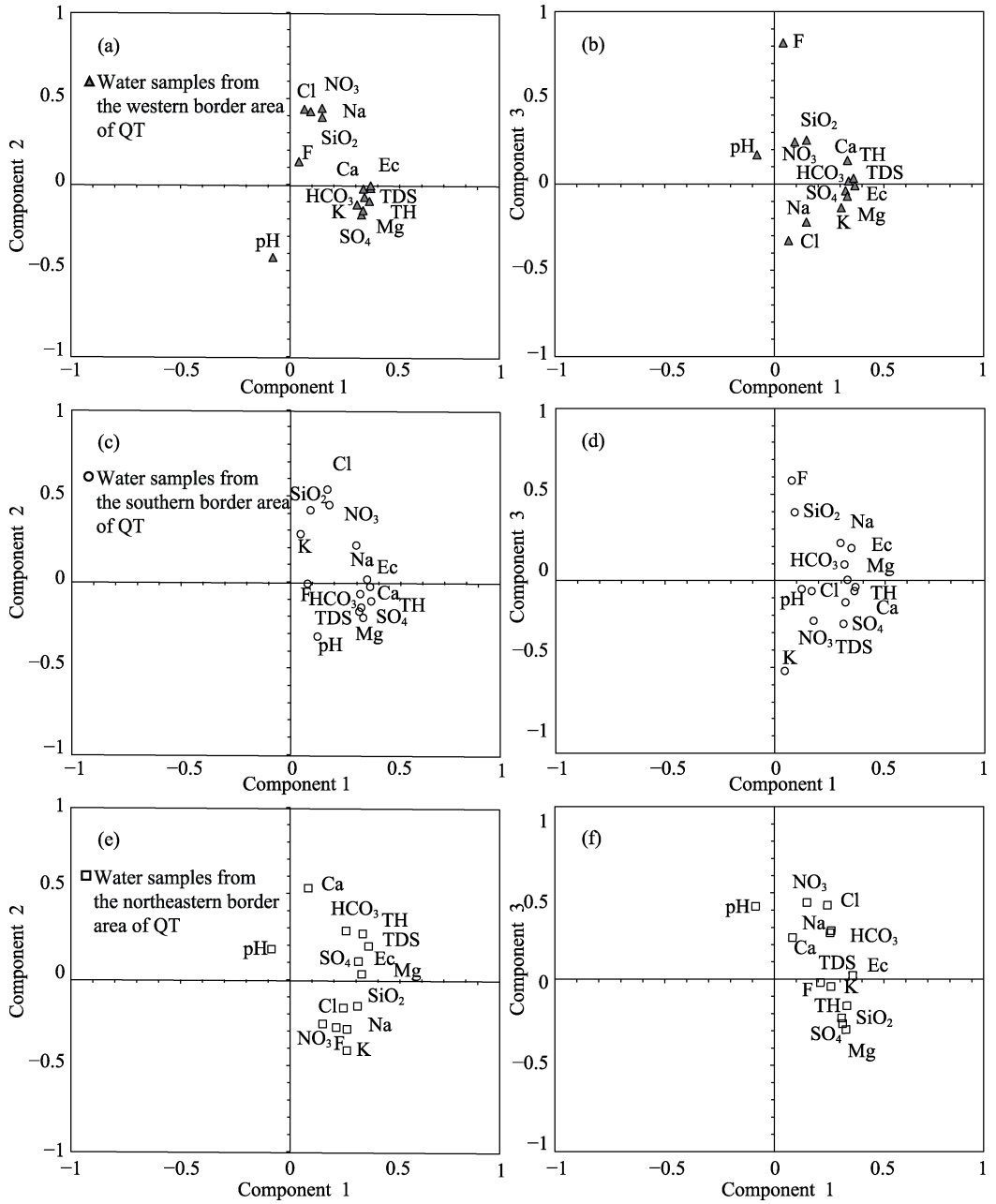

Figure 8 PCA results for variables: (a) component 1 and component 2 of water samples in the western border area, (b) component 1 and component 3 of water samples in the western border area; (c) component 1 and component 2 of water samples in the southern border area, and (d) component 1 and component 3 of water samples in the southern border area; (e) component 1 and component 2 of water samples in the northeastern border area, and (f) component 1 and component 3 of water samples in the northeastern border area of the Qinghai-Tibet Plateau

represents the geological and chemical characteristics of the rocks and soils (Meenakshi and Maheshwari, 2006).

Figures 8c and 8d show strong relationships of the southern QT border area water samples among EC, TDS, TH, Ca^{2+}, Mg^{2+}, Na^{+}, SO_4^{2-}, and HCO_3^{-} in the first component, indicating

carbonate weathering and evaporite dissolutions; K^+, Cl^- and NO_3^- in the second component, reflecting evaporite dissolutions and some anthropogenic input; and SiO_2 and F^- in the third component, showing silicate weathering and geological characteristic influence. Most of the parameters have some relationships in the first component, while only the Ca^{2+} correlation is greater in the second vector; Cl^- and NO_3^- are higher in the third vector. The correlations, predict common effects of multiple factors in the water samples of the northeastern border area of the QT (Figures 8e and 8f).

Table 5 Results of the PCA vectors, eigenvalues and % of variance

No.	West		South		Northeast	
	Eigenvalue	% of variance	Eigenvalue	% of variance	Eigenvalue	% of variance
1	7.3178	52.2703	6.9330	49.5215	6.9762	49.8304
2	3.4631	24.7362	2.1551	15.3934	2.3914	17.0814
3	1.1666	8.3326	1.4682	10.4873	1.9171	13.6934
4	0.6698	4.7843	0.9467	6.7622	1.1243	8.0310
5	0.4954	3.5387	0.7184	5.1313	0.7262	5.1872
6	0.3340	2.3859	0.7059	5.0418	0.5176	3.6968
7	0.2622	1.8729	0.4028	2.8774	0.1330	0.9501
8	0.1449	1.0349	0.3045	2.1753	0.1023	0.7308
9	0.1013	0.7236	0.2039	1.4561	0.0677	0.4835
10	0.0368	0.2627	0.0923	0.6594	0.0241	0.1724
11	0.0076	0.0542	0.0662	0.4728	0.0196	0.1397
12	0.0005	0.0037	0.0019	0.0135	0.0005	0.0034
13	0.0000	0.0000	0.0011	0.0079	0.0000	0.0000
14	0.0000	0.0000	0.0000	0.0000	0.0000	0.0000

Principal vectors are shown in bold.

4 Conclusions

In summary, through the collection, experimental measurement, and analysis of natural water samples from the three boundary areas of the QT where human activities exist, we found that water quality in the western, southern, and northeastern border areas of the QT was generally good, and most samples meet the drinking water standards. In addition, some indicators of individual water samples were even superior to the standards for drinking mineral water in China.

The QT water samples have the pH values ranging from 6.52 to 8.88, with an average of 7.75, being weakly alkaline. Furthermore, there were differences among the different boundary areas as follows: western areas (8.38), southern areas (7.57), and northeastern areas (7.66). The average TDS value in the QT water samples was 171 mg/L and the TDS were generally small. The QT water samples have the TH ranging from 3.69 mg/L (very soft) to 512 mg/L (very hard), with the average value of 168 mg/L (indicating a lower hardness).

The main cations were Ca^{2+} and Mg^{2+}, while HCO_3^- and SO_4^{2-} were the main anions. The main types of hydrochemistry in the three border areas were Ca^{2+}–Mg^{2+}–HCO_3^-– SO_4^{2-} and

Ca^{2+}–Mg^{2+}–SO_4^{2-}–HCO_3^- to the west; Ca^{2+}–Mg^{2+}–SO_4^{2-}–HCO_3^-, Ca^{2+}–Mg^{2+}– HCO_3–SO_4^{2-}, Ca^{2+}–HCO_3–SO_4^{2-}, Ca^{2+}–HCO_3^-, and Ca^{2+}–Mg^{2+}–HCO_3^- to the south; and Ca^{2+}–Mg^{2+}–HCO_3^- and Ca^{2+}–HCO_3^- to the northeast, respectively.

The genetic type of the QT border area water sample mainly was rock weathering, and the ions in the water were mainly controlled by the carbonate weathering and the evaporite dissolution; the weathering process of carbonate rocks was more intense. The main source of Cl^- in water samples of the QT border areas was the halite of the evaporites. Dissolution of sulphate minerals in the water may be among the sources of Na^+ in the western and northeastern border areas, while Na^+ in the water samples in the southern border area may have originated from silicates.

The concentration of nitrogen compounds from water samples in each boundary area from high to low were in the northeast, west, and south; this was largely consistent with the local socio-economic development level. Meanwhile, the general trend in the average concentration of sulfur compounds from high to low was in the south, east, and west. The biological quality indicators of the natural water in the border areas was far superior to GB and WHO drinking water standards, indicating that these areas have been little affected by human activities.

The regional differences in the hydrochemistry of water samples from various boundary areas mainly are the result of the combined effects of geographical environment and geological conditions. In addition, human activities have had certain effects on the regional hydrochemistry.

References

Ahmad T, Khanna P P, Chakrapani G J *et al.*, 1998. Geochemical characteristics of water and sediment of the Indus river, Trans-Himalaya, India: Constraints on weathering and erosion. *Journal of Asian Earth Sciences*, 16(2/3): 333–346.

Cao D, 2013. Yangtze River source area water environment and hydrochemistry background characteristic [D]. Beijing: Engineering China University of Geosciences (Beijing). (in Chinese)

Cao J, Zhao Y, Liu J *et al.*, 2000. Fluoride concentrations of water sources in Tibet. *Fluoride*, 33(4): 205–209.

Chang H, Xu W, Yuan J *et al.*, 2012. Current situation of grassland resources and grazing capacity in Ali, Tibet. *Pratacultural Science*, 29(11): 1660–1664. (in Chinese)

Chen J, Wang F, Xia X *et al.*, 2002. Major element chemistry of the Changjiang (Yangtze River). *Chemical Geology*, 187(3/4): 231–255.

Cruz J V L, Amaral C S, 2004. Major ion chemistry of groundwater from perched-water bodies of the Azores (Portugal) volcanic archipelago. *Applied Geochemistry*, 19(3): 445–459.

Dalai T K, Krishnaswami S, Sarin M M, 2002. Major ion chemistry in the headwaters of the Yamuna river system: Chemical weathering, its temperature dependence and CO_2 consumption in the Himalaya. *Geochimica et Cosmochimica Acta*, 66(19): 3397–3416.

Deng W, 1988. Research on fundamental characteristic of hydrochemistry in the region of the Changjiang River headwater. *Scientia Geographica Sinica*, 8(4): 363–370. (in Chinese)

Gao T, Kang S, Zhang Q *et al.*, 2008. Major ionic features and their sources in the Nam Co Basin over the Tibetan Plateau. *Environmental Science*, 29(11): 3009–3016. (in Chinese)

Gibbs R J, 1970. Mechanisms controlling world water chemistry. *Science*, 170(3962): 1088–1090.

Grange M L, Mathieu F, Begaux F *et al.*, 2001. Kashin-Beck disease and drinking water in Central Tibet. *International Orthopaedics*, 25(3): 167–169.

Guo J, Kang S, Zhang Q *et al.*, 2012. Temporal and spatial variations of major ions in Nam Co Lake water, Tibetan Plateau. *Environmental Science*, 33(7): 2295–2302. (in Chinese)

Guo Q, Wang Y, 2012. Hydrochemical anomaly of drinking waters in some endemic Kashin-Beck disease areas of

Tibet, China. *Environmental Earth Sciences*, 65(3): 659–667.

Holloway J M, Dahlgren R A, Hansen B *et al.*, 1998. Contribution of bedrock nitrogen to high nitrate concentrations in stream water. *Nature*, 395(395): 785–788.

Hou S, Xu H, An Z, 2009. Major ion chemistry of waters in Lake Qinghai catchment and the possible controls. *Earth & Environment*, 37(1): 11–19. (in Chinese)

Jin Z, Yu J, Wang S *et al.*, 2009. Constraints on water chemistry by chemical weathering in the Lake Qinghai catchment, northeastern Tibetan Plateau (China): Clues from Sr and its isotopic geochemistry. *Hydrogeology Journal*, 17(8): 2037–2048.

Ju J, Zhu L P, Wang J *et al.*, 2010. Water and sediment chemistry of Lake Pumayum Co, South Tibet, China: Implications for interpreting sediment carbonate. *Journal of Paleolimnology*, 43(3): 463–474.

Katz B G, Böhlke J K, Hornsby H D, 2001. Timescales for nitrate contamination of spring waters, northern Florida, USA. *Chemical Geology*, 179(1–4): 167–186.

Li S, Wang M, Yang Q *et al.*, 2012. Enrichment of arsenic in surface water, stream sediments and soils in Tibet. *Journal of Geochemical Exploration*, 135(6): 104–116.

Li S, Yang L, Wang W *et al.*, 2006. Study on the relationship between selenium concentrations in drinking water and Kaschin-Beck Disease in Tibet. *Chinese Journal of Endemiology*, 25(4): 428–429. (in Chinese)

Li S, Zhang Q, 2008. Geochemistry of the upper Han River basin, China, 1: Spatial distribution of major ion compositions and their controlling factors. *Applied Geochemistry*, 23(12): 3535–3544.

Lu Y, Li Y, Mimapuchi *et al.*, 2016. Evolution of structural geology and metallogenic unite, Xizang (Tibet) Autonomous Region. *Geological Review*, 62(b11): 219–220. (in Chinese)

Meenakshi, Maheshwari R C, 2006. Fluoride in drinking water and its removal. *Journal of Hazardous Materials*, 137(1): 456–463.

Meybeck M, 1987. Global chemical weathering of surficial rocks estimated from river dissolved loads. *American Journal of Science*, 287(5): 401–428.

Meybeck M, Helmer R, 1989. The quality of rivers: From pristine stage to global pollution. *Palaeogeography Palaeoclimatology Palaeoecology*, 75(4): 283–309.

Ministry of Environment Protection of the People's Republic of China (MEP), 2002. Methods for Chemical Analysis of Water and Waste Water. Beijing: China Environmental Science Press. (in Chinese)

Ministry of Health of the People's Republic of China (MH), 2007. Standards Examination Methods for Drinking Water GB/T 5750–2006. Beijing: China Standards Press. (in Chinese)

Ministry of Health of the People's Republic of China (MH), 2007. Standards for Drinking Water Quality GB 5749–2006. Beijing: China Standards Press. (in Chinese)

National Bureau of Statistics of People's Republic of China (NBS), 2017. China Statistical Yearbook 2017. Beijing: China Statistics Press. (in Chinese)

Nemeth A, Paolini J, Herrera R, 1982. Carbon transport in the Orinoco River: The preliminary results. Nairobi, Kenya, Scientific Committee on Problems of the Environment/United Nations Environment Programme Sonderband Heft.

Nie L, 2011. Analysis of microbial indicators of drinking water in rural areas of six counties in Tibet. *Tibet Medical Journal*, 32(1): 56–57. (in Chinese)

Piper A M, 1944. A graphic procedure in the geochemical interpretation of water-analyses. *Eos*, *Transactions American Geophysical Union*, 25(6): 914–928.

Reeder S W, Hitchon B, Levinson A A, 1972. Hydrogeochemistry of the surface waters of the Mackenzie River drainage basin, Canada (I): Factors controlling inorganic composition. *Geochimica et Cosmochimica Acta*, 36(8): 825–865.

Roy S, Gaillardet J, Allègre C J, 1999. Geochemistry of dissolved and suspended loads of the Seine River, France: Anthropogenic impact, carbonate and silicate weathering. *Geochimica et Cosmochimica Acta*, 63(9): 1277–1292.

Sarin M M, Krishnaswami S, 1984. Major ion chemistry of the Ganga–Brahmaputra river systems, India. *Nature*, 312(5994): 538–541.

Sarin M M, Krishnaswami S, Dilli K *et al.*, 1989. Major ion chemistry of the Ganga-Brahmaputra river system: Weathering processes and fluxes to the Bay of Bengal. *Geochimica et Cosmochimica Acta*, 53(5): 997–1009.

Shen Z, Zhu W, Zhong Z, 1993. Hydrogeochemical Basis. Beijing: Geological Publishing House. (in Chinese)

Sheng Y, Rui Y, Yu Y, 2012. Heavy metal pollution in water of rivers and lake in Tibet by ICP-MS. *Asian Journal of Chemistry*, 24(11): 5403–5404.

Sun H, Zheng D, Yao T *et al.*, 2012. Protection and construction of the national ecological security shelter zone on Tibetan Plateau. *Acta Geographica Sinica*, 67(1): 3–12. (in Chinese)

Sun R, Zhang X, Wu Y, 2012. Major ion chemistry of water and its controlling factors in the Yamzhog Yumco Basin, South Tibet. *Journal of Lake Sciences*, 24(4): 600–608. (in Chinese)

Sun R, Zhang X, Zheng D, 2013. Spatial variation and its causes of water chemical property in Yamzhog Yumco Basin, South Tibet. *Acta Geographica Sinica*, 68(1): 36–44. (in Chinese)

Tan L, Li F, Li Z *et al.*, 2016. Study on groundwater characteristics and development in permafrost region of Tuotuo River. *Yellow River*, 38(5): 62–67. (in Chinese)

Tian Y, Yu C, Luo K *et al.*, 2015. Hydrochemical characteristics and element contents of natural waters in Tibet, China. *Journal of Geographical Sciences*, 25(6): 669–686.

Tian Y, Yu C, Zha X *et al.*, 2016. Distribution and potential health risks of arsenic, selenium, and fluorine in natural waters in Tibet, China. *Water*, 8(12): 568.

United States Environmental Protection Agency (EPA), 1993. Determination of inorganic anions by ion chromatography. Cincinnati, Ohio 45268, Environmental Protection Agency Environmental Monitoring Systems Laboratory Office of Research and Decelopment.

Wang J, Ju J, Zhu L, 2013. Water chemistry variations of lake and inflowing rivers between pre- and post-monsoon season in Nam Co, Tibet. *Scientia Geographica Sinica*, 33(1): 90–96. (in Chinese)

Wang L, 2016. Study on hydrochemical characteristics and its influencing factors in Yarlung Tsangpo River Basin [D]. Beijing: University of Chinese Academy of Sciences. (in Chinese)

Wang M, Li S, Wang H *et al.*, 2012. Distribution of arsenic in surface water in Tibet. *Environmental Science*, 33(10): 3411–3416. (in Chinese)

World Health Organization (WHO), 2008. Guidelines for drinking-water quality. Geneva, World Health Organization**:** 186.

Wu W, Yang J, Xu S *et al.*, 2008. Geochemistry of the headwaters of the Yangtze River, Tongtian He and Jinshajiang: Silicate weathering and CO consumption. *Applied Geochemistry*, 23(12): 3712–3727.

Xiao J, Jin Z, Zhang F *et al.*, 2012. Major ion geochemistry of shallow groundwater in the Qinghai Lake catchment, NE Qinghai-Tibet Plateau. *Environmental Earth Sciences*, 67(5): 1331–1344.

Yao T, Thompson L G, Qin D *et al.*, 1996. Variations in temperature and precipitation in the past 2000 a on the Xizang (Tibet) Plateau–Guliya ice core record. *Science in China* (*Series D*), 39(4): 425–433.

Yao Z, Rui W, Liu Z *et al.*, 2015. Spatial-temporal patterns of major ion chemistry and its controlling factors in the Manasarovar Basin, Tibet. *Journal of Geographical Sciences*, 25(6): 687–700.

Zhang M, Gustafsson J E, 1995. The Tibetan Water Environment: Water Chemistry of Some Surface Waters in Southern Tibet. *Ambio*, 24(6): 385–387.

Zhang X, He Y, Shen Z *et al.*, 2015. Frontier of the ecological construction support the sustainable development in Tibet Autonomous Region. *Bulletin of Chinese Academy of Sciences*, (3): 306–312. (in Chinese)

Zhang X, Li X, Budu *et al.*, 2013. Analysis on sanitary surveillance of drinking water quality in Nyingchi region of Tibet in 2011. *Tibet Medical Journal*, 34(1): 62–64. (in Chinese)

Zhang X, Sun R, Zhu L, 2012. Lake water in the Yamzhog Yumco basin in south Tibetan region: Quality and evaluation. *Journal of Glaciology and Geocryology*, 34(4): 950–958. (in Chinese)

Zhang Y, Li B, Zheng D, 2002. A discussion on the boundary and area of the Tibetan Plateau in China. *Geographical Research*, 21(1): 1–8. (in Chinese)

Zhao T, Chen Y, Yao W *et al.*, 2017. The spatiotemporal distribution of two bacterial indexes in a small Tibetan Plateau watershed. *Water*, 9(11): 823.

Zhe M, Zhang X, Wang B *et al.*, 2017. Hydrochemical regime and its mechanism in Yamzhog Yumco Basin, South Tibet. *Journal of Geographical Sciences*, 27(9): 1111–1122.

Zheng D, Tan J, Wang W, 2007. Environmental Geosciences Introduction. Beijing: Higher Education Press.

Zhu B, Yang X, 2007. Chemical characteristics and origin of natural water in the Taklimakan Desert. *Chinese Science Bulletin*, 52(13): 1561–1566. (in Chinese)

Zhu L, Ju J, Yong W *et al.*, 2010. Composition, spatial distribution, and environmental significance of water ions in Pumayum Co catchment, southern Tibet. *Journal of Geographical Sciences*, 20(1): 109–120.